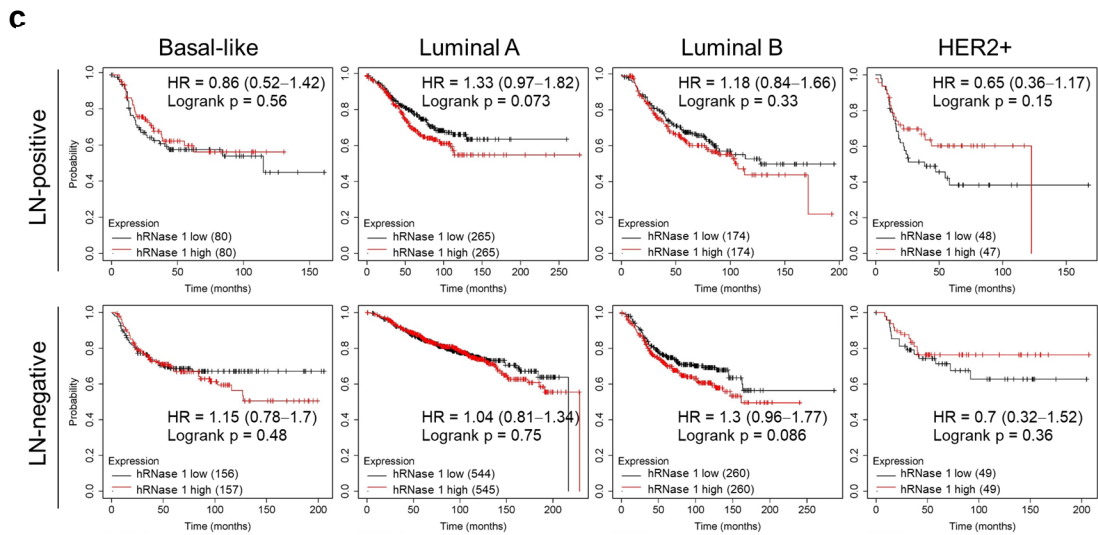
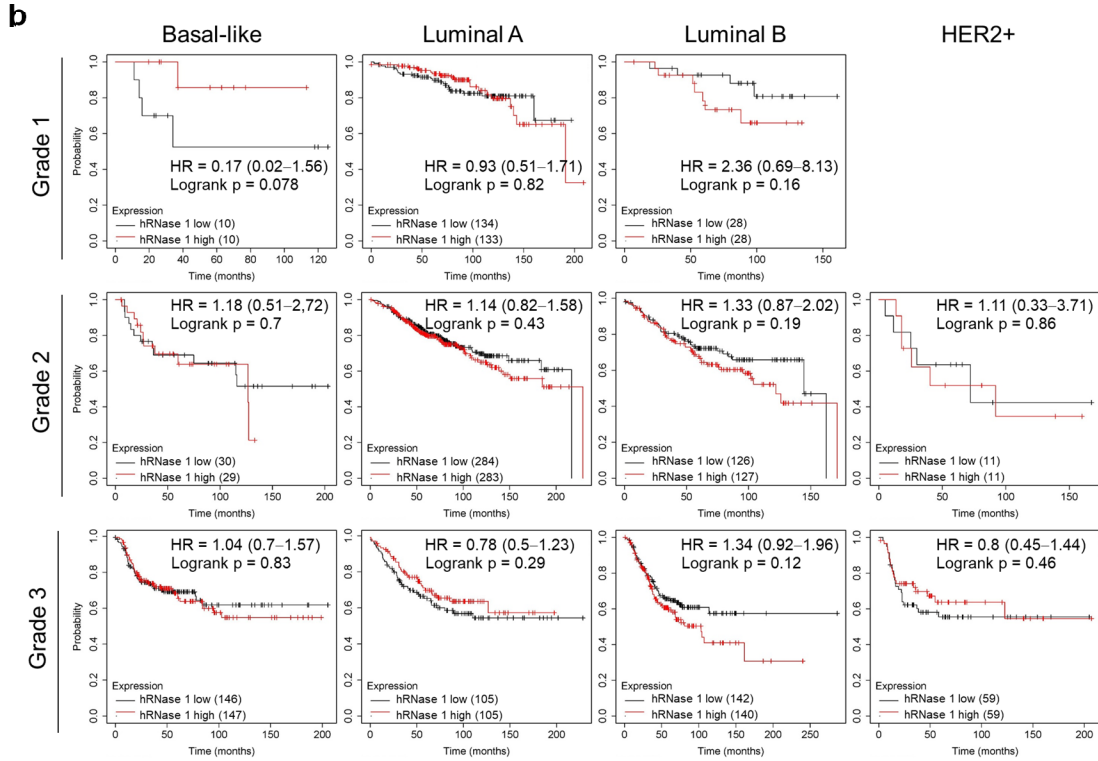
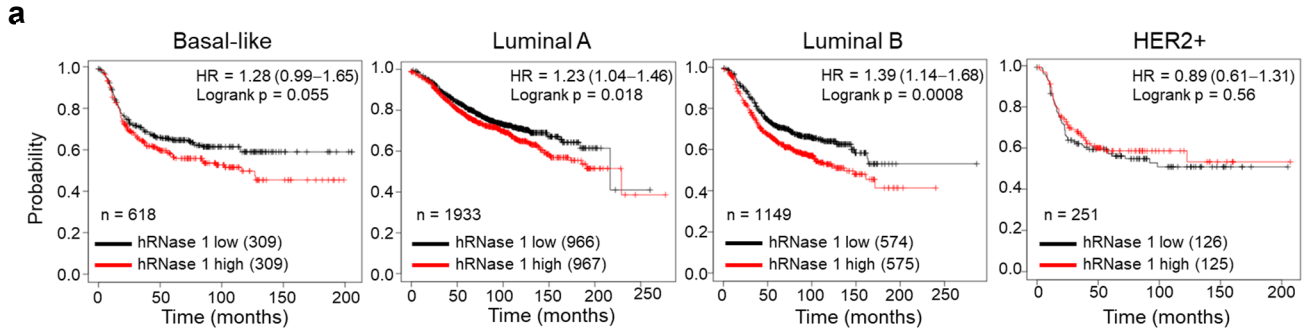
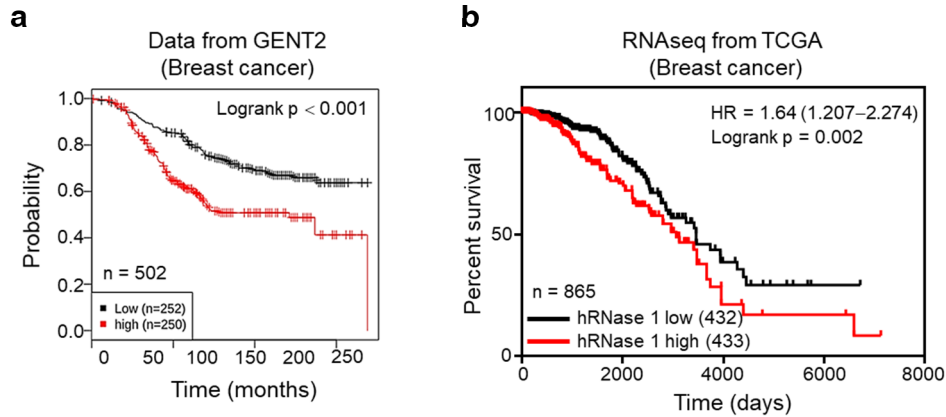


Supplementary Fig. 1. Survival curve analysis by screening the expression of hRNase family in human cancers. a and b, Prognostic correlation of survival analyses of breast cancer patients with high and low hRNases expression as indicated. Data was analyzed from the overall survival (a; OS) and the relapse free survival (b; RFS). Survival data were analyzed using Kaplan-Meier Plotter [Probe: 206111_at (hRNase 2); 206851_at (hRNase 3); 205158_at (hRNase 4); 205141_at

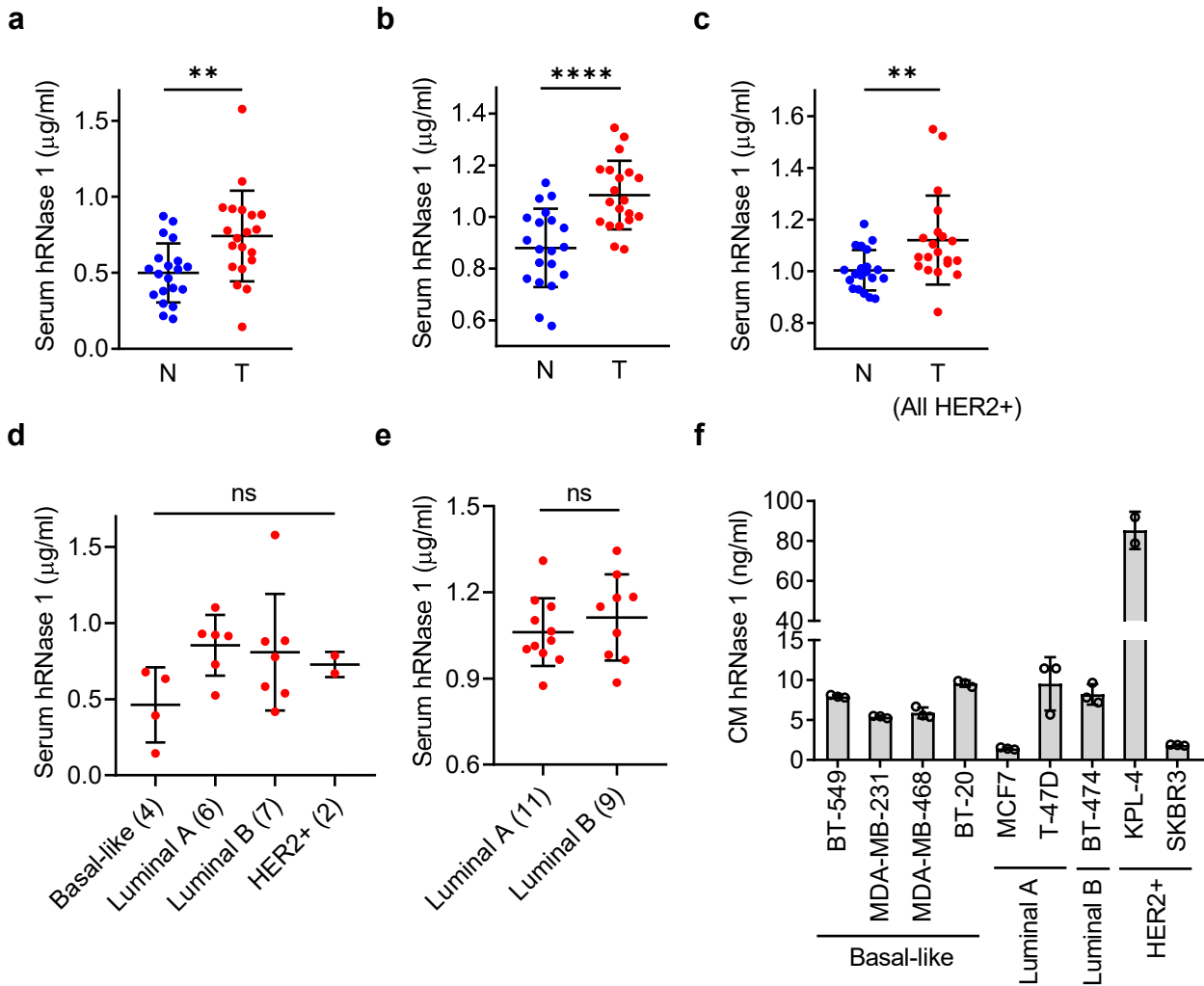
(hRNase 5); 213566_at (hRNase 6); 234699_at (hRNase 7); 231603_at (hRNase 11)]. HR, hazard ratio. All p values are calculated by Log-rank test.



Supplementary Fig. 2. High hRNase 1 expression correlates with poor patient survival in breast cancer patients with basal-like, luminal A, and luminal B subtypes. a, Prognostic correlation of the RFS of breast cancer patients in different breast cancer subtypes with different hRNase 1 levels as indicated. **b and c,** Prognostic correlation of the RFS of breast cancer patients with different grades (**b**) and lymph node (LN) statuses (**c**) in different breast cancer subtypes with different hRNase 1 levels as indicated. Data of grade 1 patients with of HER2+ is not provided in the database. All p values are calculated by Log-rank test (**a–c**).

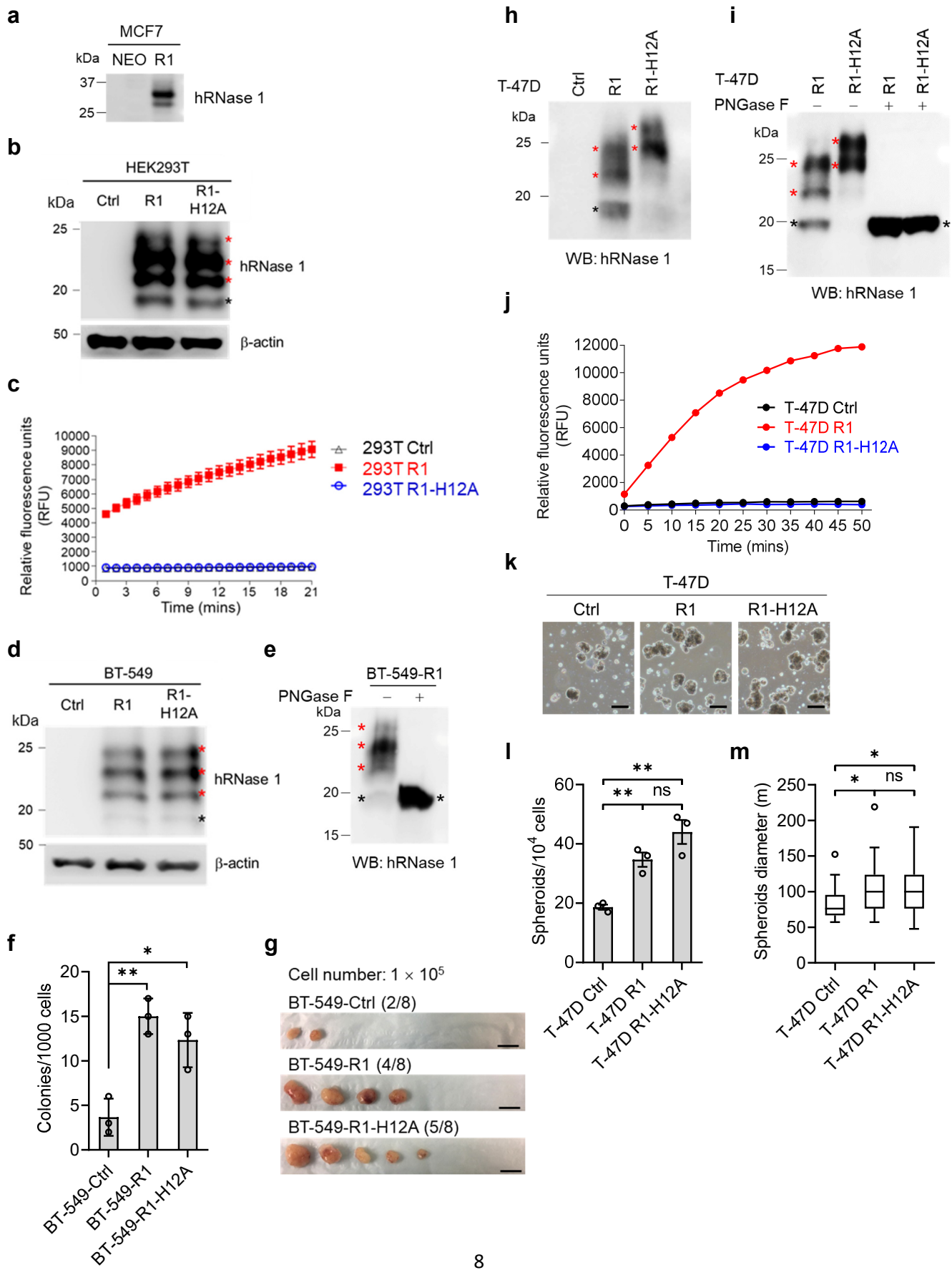


Supplementary Fig. 3. High hRNase 1 expression correlates with poor patient survival in two other independent databases of patients with breast cancer. **a**, Prognostic correlation of the OS of breast cancer patients with high and low hRNase 1 expression divided by the median value, analyzed the Kaplan-Meier Plotter from the GENT2 database (<http://gent2.appex.kr/gent2/>). **b**, Prognostic correlation of the OS of breast cancer patients with high and low hRNase 1 expression divided by the median value, analyzed the Kaplan-Meier survival curve from the UCSC Cancer Genome Browser (<http://xena.ucsc.edu/welcome-to-ucsc-xena/>) using the interpreted expression profile of TCGA breast invasive carcinoma by RNA sequencing (dataset ID: TCGA_BRCA_exp_HiSeqV2). Both p values are calculated by Log-rank test (**a**, **b**).



Supplementary Fig. 4. Serum samples of breast cancer patients show higher hRNase 1 expression than normal individuals. a–c, ELISA of hRNase 1 levels in three independent cohorts of serum samples of breast tumor patients (T; n = 20) compared with noncancerous individuals (N; n = 20). **p = 0.0041, **p < 0.0001, **p = 0.0090, respectively. All patients in the cohort (c) belong to HER2+ subtype. d, ELISA of hRNase 1 levels in breast tumor serum samples from (a) subdivided into four molecular subtypes, including Basal-like (n = 4), Luminal A (n = 6), Luminal B (n = 7), and HER2+ (n = 2). e, ELISA of hRNase 1 levels in breast tumor serum samples from (b) subdivided into two molecular subtypes, including Luminal A (n = 11) and Luminal B (n**

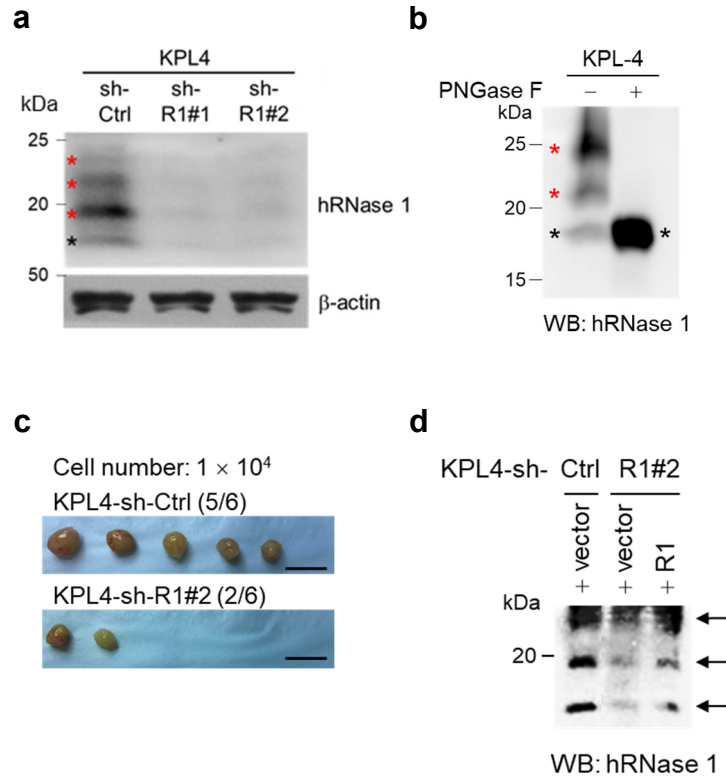
= 9). **f**, ELISA of hRNase 1 expression in the conditioned medium (CM) of breast cancer cells. Data represent three independent experiments. All error bars represent mean \pm SD. ** $p < 0.01$, **** $p < 0.0001$, ns, not significant, two-tailed unpaired t test (**a**, **b**, **c**, **e**), One way ANOVA analysis (**d**). Source data are provided as a Source Data file.



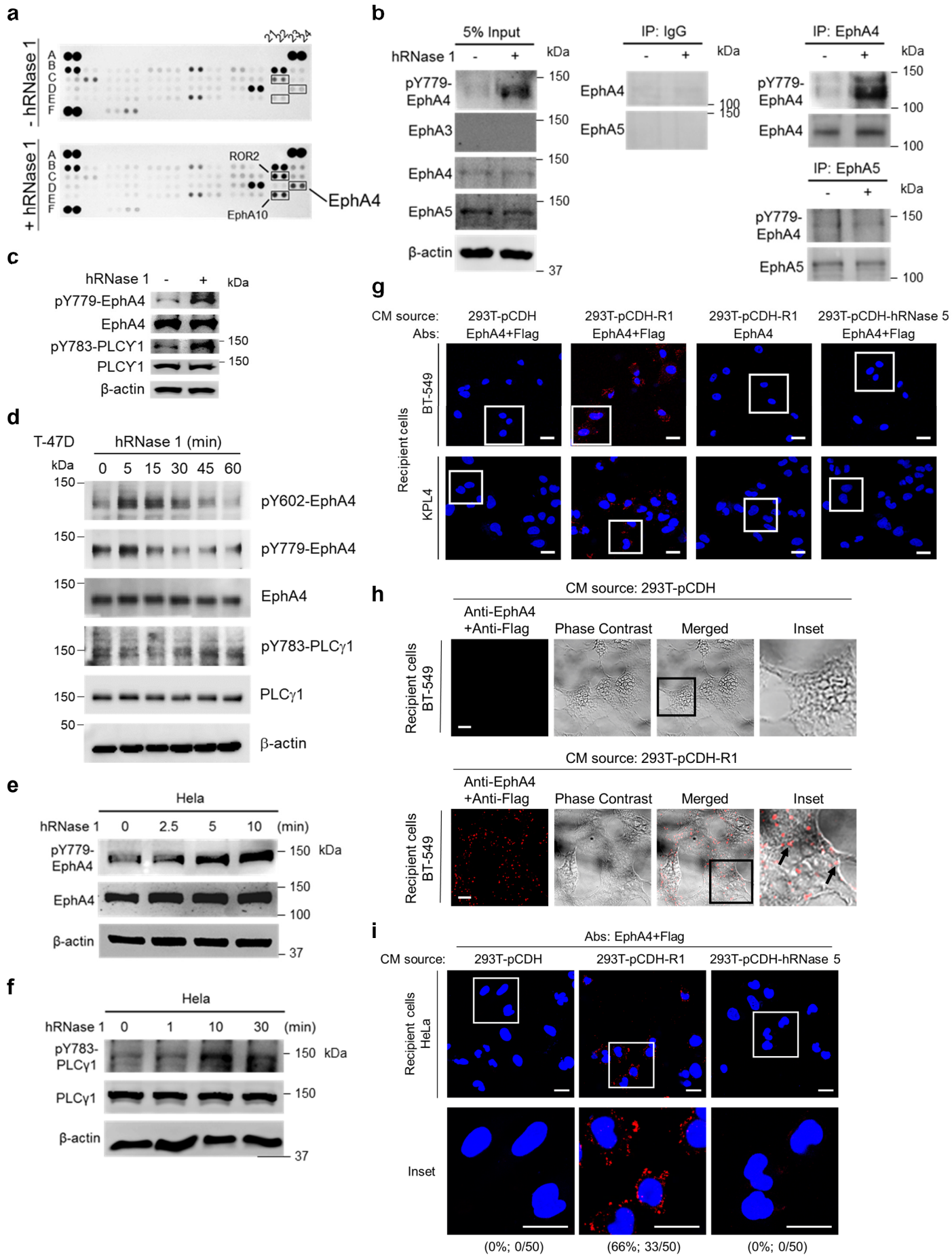
Supplementary Fig. 5. hRNase 1 increases the sphere-forming ability and enhances the tumor-initiating capability of breast cancer cells independently of its ribonucleolytic activity.

a, WB of secreted proteins from CM in MCF7 control cells (MCF7-NEO) and hRNase 1 expressing MCF7 cells (MCF7-R1) with hRNase 1 antibody. **b**, WB of cell lysates in Flag-tagged hRNase 1 in HEK293T transfected with an empty control vector (Ctrl), R1, and R1-H12A with Flag and β -actin antibodies. **c**, Analysis of RNase enzymatic activity by an RNaseAlert® Lab Test kit in CM collected from HEK293T transfected with the indicated plasmids. Data are representative of two independent experiments in triplicate. Error bars represent mean \pm SD. **d**, WB of cell lysates in BT-549 stable transfectants expressing empty control (Ctrl), R1, and R1-H12A with Flag and β -actin antibodies. **e**, WB of secreted proteins from CM in BT-549-R1 treated without or with PNGase F. **f**, Quantification of soft agar colony formation assay of cells from **(d)**. Ctrl vs R1, ** $p = 0.002$, Ctrl vs R1-H12A, * $p = 0.015$. **g**, Representative images of limiting dilution assay of the indicated BT-549 stable clones (1×10^5) from Figure 2g. The number of tumor-forming mice within each group is shown in the parentheses. Bar, 1 cm. **h**, WB of secreted proteins from CM in T-47D stable transfectants expressing empty control (Ctrl), R1, and R1-H12A with hRNase 1 antibody. **i**, WB of secreted proteins from CM in T-47D R1 and T-47D R1-H12A treated without or with PNGase F. **j**, Analysis of RNase enzymatic activity by an RNaseAlert® Lab Test kit in CM collected from **(h)**. **k**, Representative images of primary spheres from **(h)**. Bar, 100 μ m. **l** and **m**, Quantification of spheroid number (**l**) and diameter (**m**) of spheroid formation assay from **(h)**. **l**, Ctrl vs R1, ** $p = 0.0033$, Ctrl vs R1-H12A, ** $p = 0.0036$. **m**, Ctrl vs R1, * $p = 0.0296$, Ctrl vs R1-H12A, * $p = 0.0497$. Box plots, including T-47D Ctrl ($n = 23$), T-47D R1 ($n = 30$), and T-47D R1-H12A ($n = 36$), indicate minima (lower end of whisker), maxima (upper end of whisker), median (centre), 25th percentile (bottom of box) and 75th percentile (top of box) as well as outliers

(single points) (**m**). Error bars represent mean \pm SD (**f**) and mean \pm SEM (**l**), n = 3 independent experiments (**f**, **l**). *p < 0.05, **p < 0.01, ns, not significant, two-tailed unpaired t test (**f**, **l**, **m**). Each experiment was repeated a second time with similar results (**a**, **b**, **d**, **e**, **h**, **i**). Antibodies used in WB, hRNase 1 (Sigma-Aldrich, #HPA001140); Flag (Sigma-Aldrich, #F3165); β -actin (Sigma-Aldrich, #A2228). Red asterisk, glycosylated hRNase 1; black asterisk, non-glycosylated hRNase 1. Source data are provided as a Source Data file.



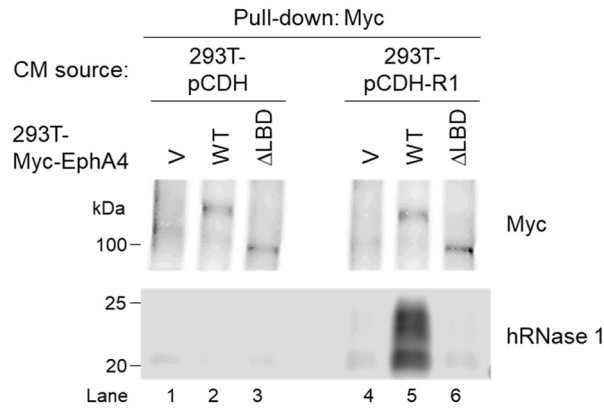
Supplementary Fig. 6. Silencing hRNase 1 decreases the tumor-initiating capability in KPL4 cells. **a**, WB of cell lysates in KPL4 stable transfectants knocking down hRNase 1 and empty control with hRNase 1 and β -actin antibodies. **b**, WB of secreted proteins from CM in KPL4 treated without or with PNGase F. **c**, Representative images of limiting dilution assay of the indicated KPL4 stable clones (1×10^4) from Figure 2j. The number of tumor-forming mice within each group is shown in the parentheses. Bar, 1 cm. **d**, WB of secreted proteins from CM in the reconstitution of vector control or hRNase 1 in hRNase 1-knockdown KPL4 (KPL4-sh-R1#2) and control cells (KPL4-sh-Ctrl). Each experiment was repeated a second time with similar results (**a**, **b**, **d**). Antibodies used in WB, hRNase 1 (Sigma-Aldrich, #HPA001140); β -actin (Sigma-Aldrich, #A2228). Red asterisk, glycosylated hRNase 1; black asterisk, non-glycosylated hRNase 1. Source data are provided as a Source Data file.



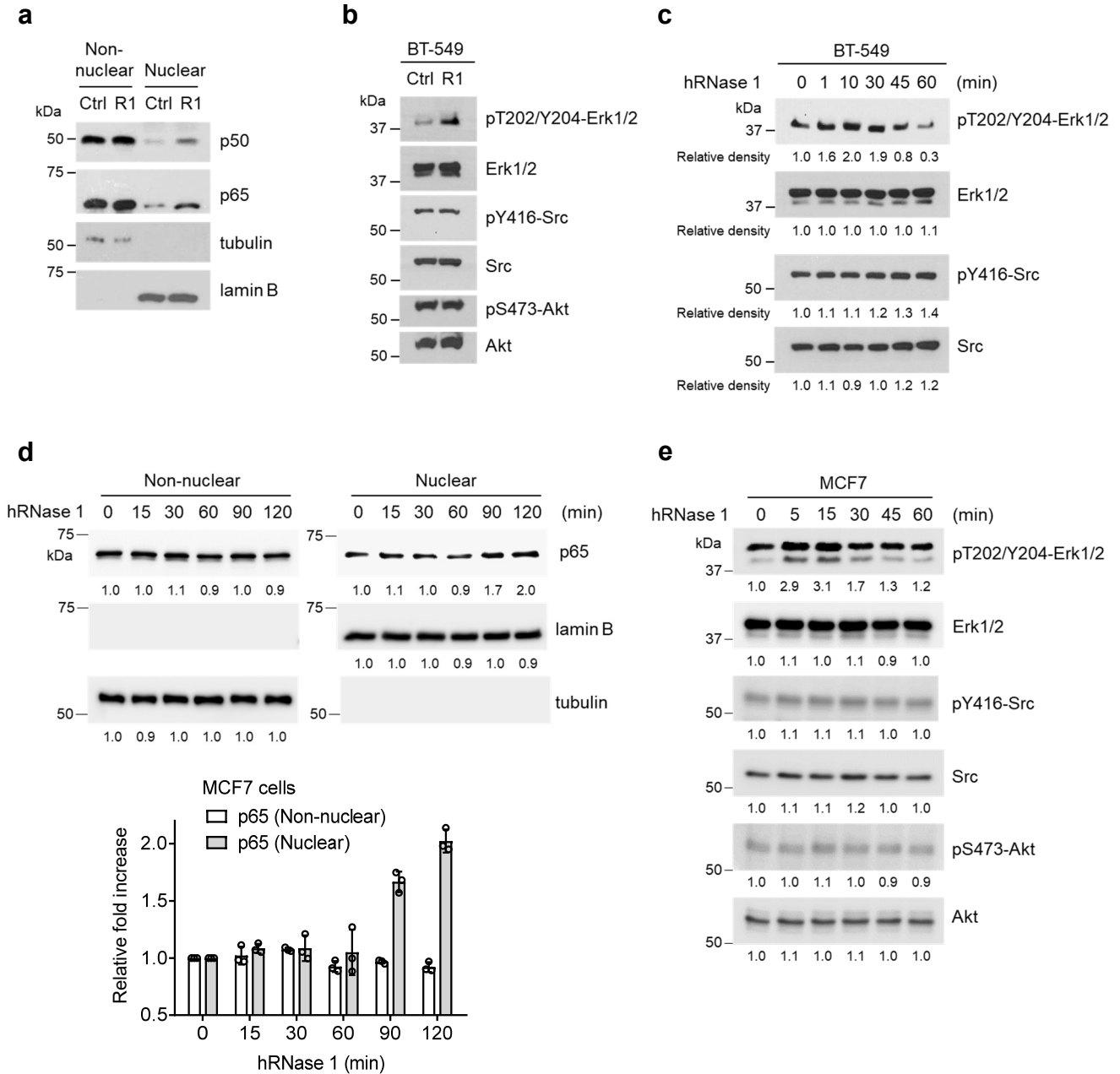
Supplementary Fig. 7. hRNase 1 stimulates EphA4 signaling and interacts with EphA4 in several cancer cell lines. **a**, Human phospho-RTK antibody array analysis of BT-549 cells treated with or without recombinant hRNase 1 protein purified from HEK293 cells (1 $\mu\text{g/ml}$) for 30 min after serum starvation for 3 hr. Three pairs of positive signals in duplicate coordinates (- hRNase 1 comparing to + hRNase 1) are shown in EphA4 (D23/D24), EphA10 (E21/E22), and ROR2 (C21/C22). **b**, Immunoprecipitation (IP) of BT-549 cells treated with or without 1 $\mu\text{g/ml}$ hRNase 1 for 30 min, followed by WB with the indicated antibodies. Immunoglobulin G (IgG) was used as a control for IP. **c**, WB of BT-549 cells treated with or without hRNase 1 for 30 min with the indicated antibodies. **d**, WB of T-47D cells treated with or without hRNase 1 at various time points with the indicated antibodies. **e** and **f**, WB of pY779-EphA4 and EphA4 (**e**) as well as pY783-PLC γ 1 and PLC γ 1 (**f**) in HeLa cells treated with hRNase 1 (1 $\mu\text{g/ml}$) at different time points as indicated. **g**, Duolink *in situ* proximity ligation assay (PLA) of BT-549 and KPL4 cells, treated with CM collected from 293T-pCDH, 293T-pCDH-R1, or 293T-pCDH-hRNase 5 for 30 min, and stained with EphA4 only or EphA4 plus Flag antibodies as indicated. Insets for Figure 3f, BT-549, enlargements of the boxed areas at 9 \times magnification; KPL4, enlargements of the boxed areas at 12.25 \times magnification. Bar, 25 μm . **h**, Duolink *in situ* PLA of BT-549 cells, treated with CM collected from 293T-pCDH or 293T-pCDH-R1 for 30 min, and stained with EphA4 and Flag antibodies. Arrows in the insets, red dots, positive Duolink *in situ* signals. Insets, enlargements of the boxed areas (6 \times magnification). Bar, 10 μm . **i**, Duolink *in situ* PLA of HeLa cells, treated with CM collected from 293T-pCDH, 293T-pCDH-R1, or 293T-pCDH-hRNase 5 for 30 min, and stained with EphA4 and Flag antibodies. Inset, 9 \times magnification. Bar, 25 μm . The quantified results in the parentheses showing the percentage of cells with positive PLA signals calculated

from a pool of 50 cells. Each experiment was repeated an additional time with similar results (**a–i**).

Source data are provided as a Source Data file.



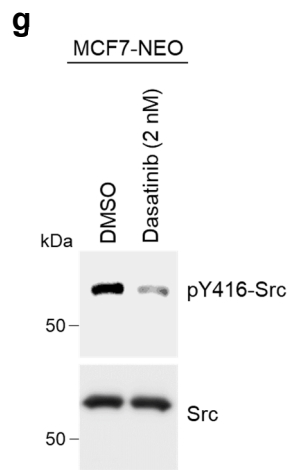
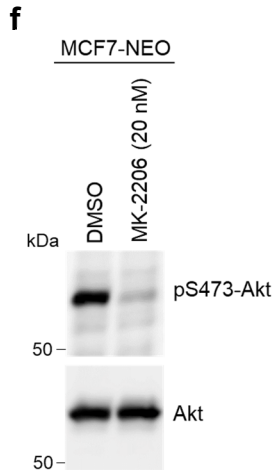
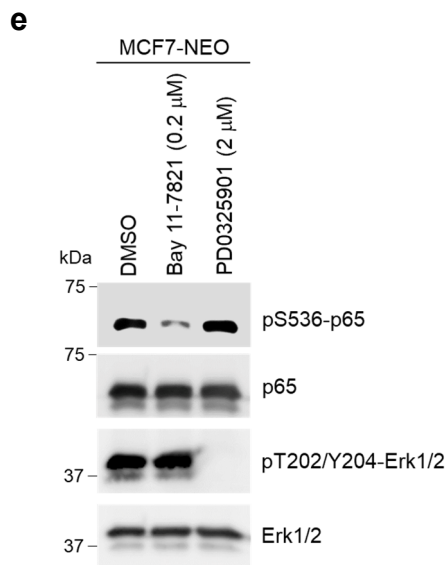
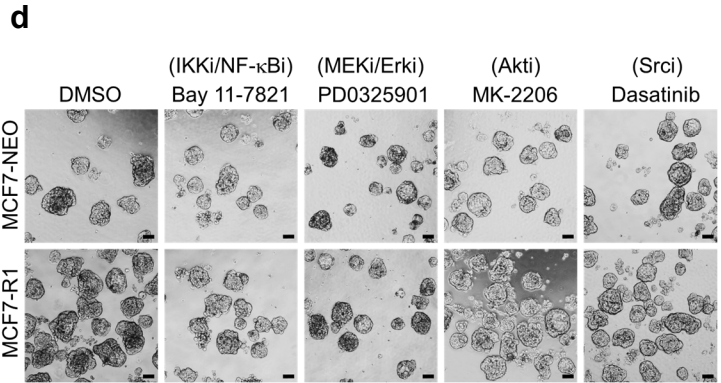
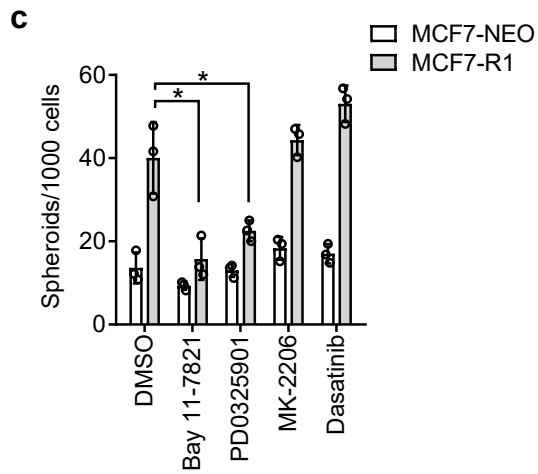
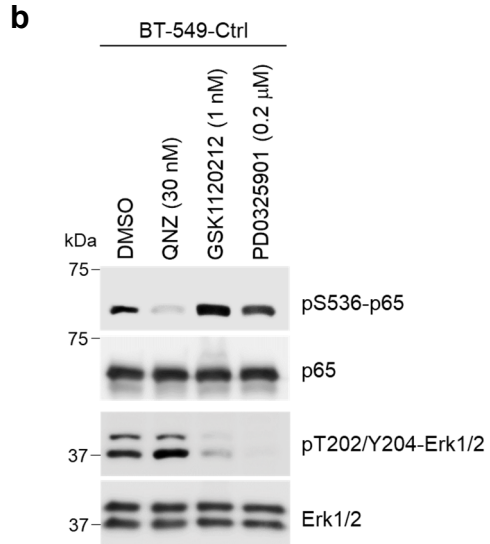
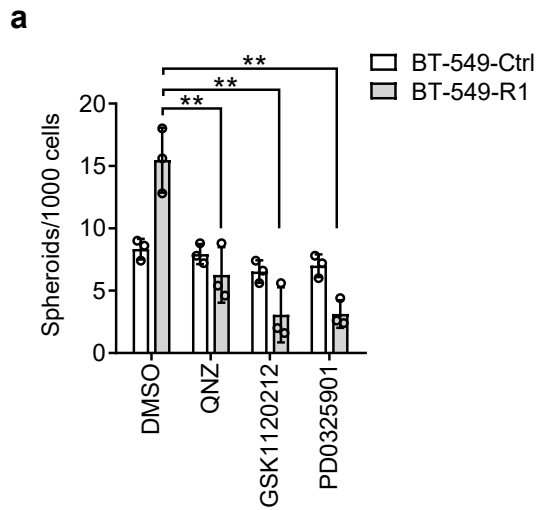
Supplementary Fig. 8. The extracellular ligand-binding domain of EphA4 is critical for hRNase 1 binding. *In vitro* binding assay of 293T stable transfectants with empty vector (V), Myc-tagged EphA4 containing wild-type (WT), and ligand-binding domain deletion (ΔLBD), incubated with CM collected from 293T stable transfectant expressing empty vector (293T-pCDH) or Flag-tagged hRNase 1 (293T-pCDH-R1). Data are representative of two independent experiments with similar results. Source data are provided as a Source Data file.



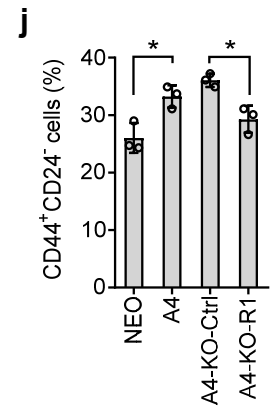
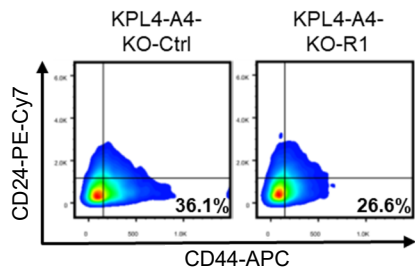
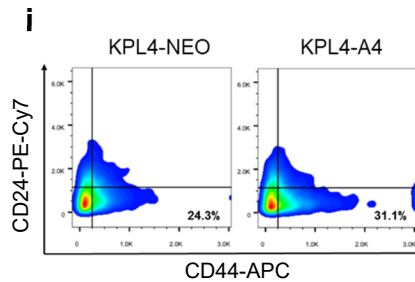
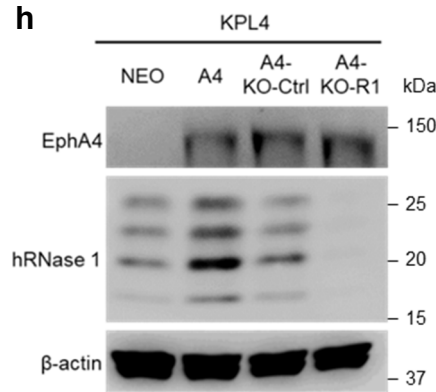
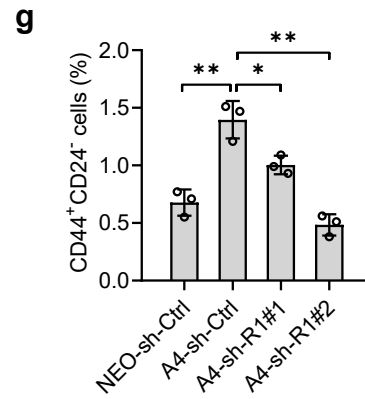
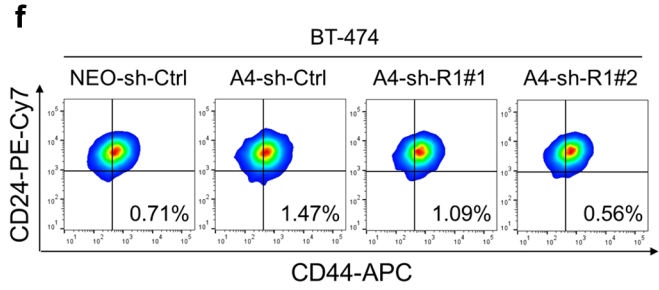
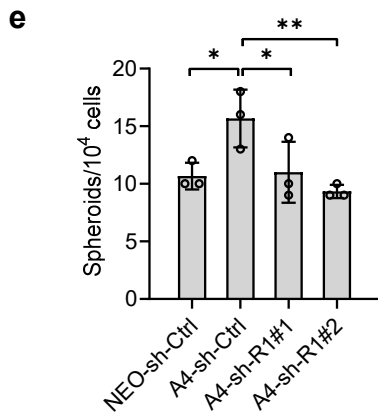
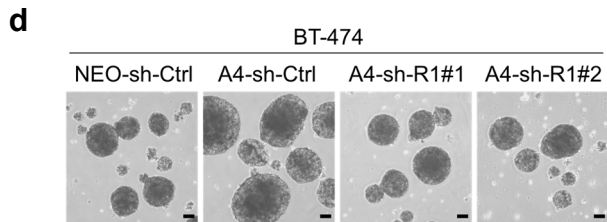
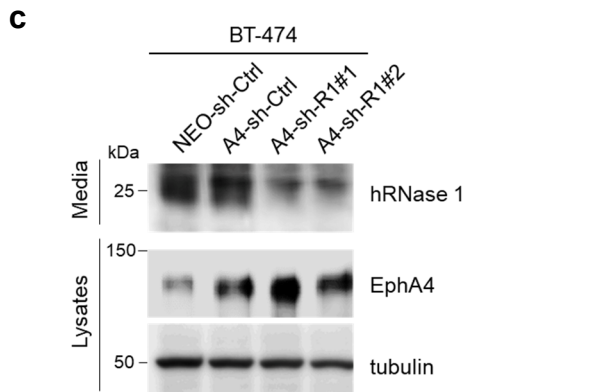
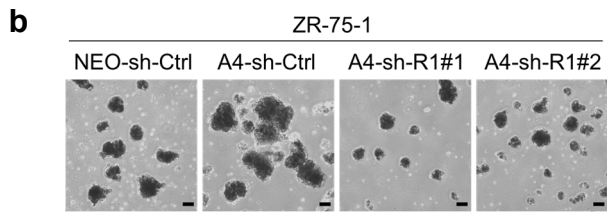
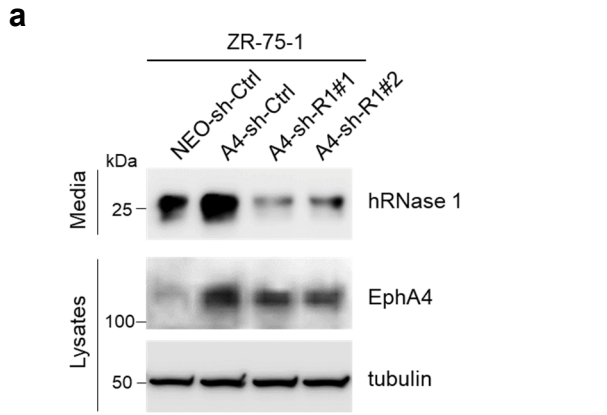
Supplementary Fig. 9. hRNase 1 activates signaling pathways of NF- κ B and Erk, but not Src

or Akt, in BT-549 and MCF7 cells. a, Cellular fractionation of BT-549-Ctrl and BT-549-R1 stable clones, followed by WB with the indicated antibodies. Tubulin and lamin B were used as markers for the non-nuclear and nuclear portions, respectively. **b**, WB of BT-549-Ctrl and BT-549-R1 stable clones with the indicated antibodies. **c**, WB of BT-549 cells treated with

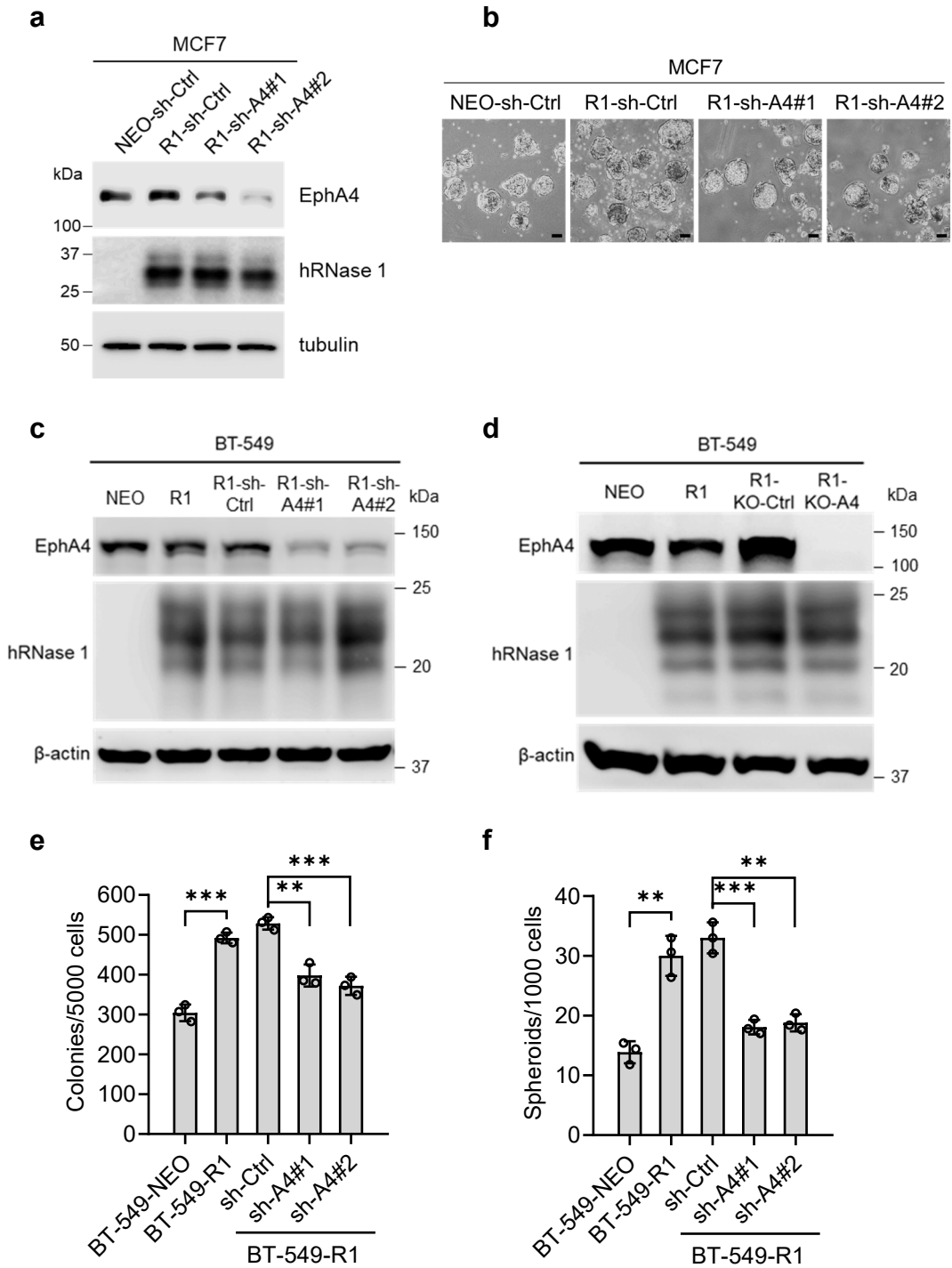
recombinant hRNase 1 protein purified from HEK293 cells (1 $\mu\text{g/ml}$) at various time points with the indicated antibodies. **d**, Top, cellular fractionation of MCF7 cells treated with hRNase 1 (1 $\mu\text{g/ml}$) at various time points, followed by WB with the indicated antibodies. Bottom, quantification of fold increase normalized against that at time 0 min. Error bars represent mean \pm SD, n = 2 independent experiments. **e**, WB of MCF7 cells treated with hRNase 1 (1 $\mu\text{g/ml}$) at various time points with the indicated antibodies. Relative density of signals were quantified using ImageJ. Data are representative of two (**a**) or three (**b**, **c**, **e**) independent experiments with similar results. Source data are provided as a Source Data file.



Supplementary Fig. 10. hRNase 1 induces spheroid formation via the MEK/Erk and IKK/NF- κ B activation pathways in BT-549 and MCF7 cells. **a**, Quantification of spheroid formation assay in BT-549-Ctrl and BT-549-R1 stable clones incubated with the inhibitors against IKK/NF- κ B (QNZ, 30 nM) and MEK/Erk (GSK1120212, 1 nM; PD0325901, 0.2 μ M). DMSO vs QNZ, ** $p = 0.0097$, DMSO vs GSK1120212, ** $p = 0.0032$, DMSO vs PD0325901, $p = **0.0016$. **b**, WB of BT-549-Ctrl cells treated with DMSO or various inhibitors for 1 day with the indicated antibodies. **c**, Quantification of spheroid formation assay in MCF7-NEO and MCF7-R1 stable clones incubated with the inhibitors against IKK/NF- κ B (Bay 11-7821, 0.2 μ M), MEK/Erk (PD0325901, 2 nM), Akt (MK-2206, 20 nM), and Src (Dasatinib, 2 nM). DMSO vs Bay 11-7821, * $p = 0.0133$, DMSO vs PD0325901, $p = *0.0275$. **d**, Representative images of sphere formation assay from (c). Bar, 100 μ m. **e–g**, WB of MCF7-NEO cells treated with DMSO or various inhibitors for 1 day with the indicated antibodies. Error bars represent mean \pm SD. Data are representative of two (b, e–g) or three (a, c, d) independent experiments. * $p < 0.05$, ** $p < 0.01$, two-tailed unpaired t test. Source data are provided as a Source Data file.

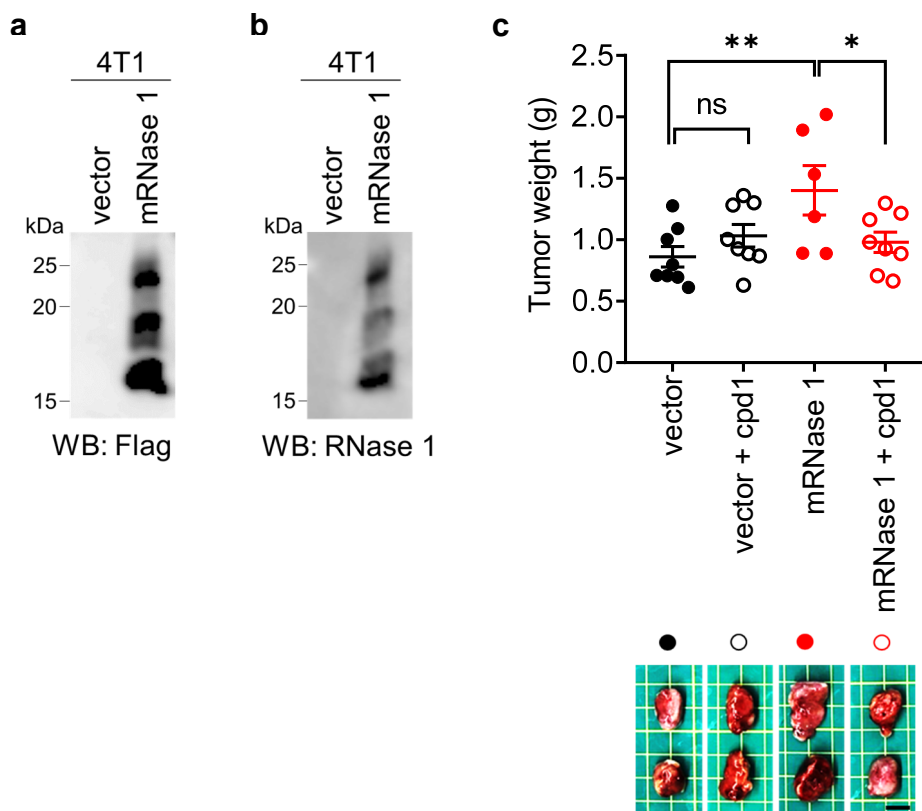


Supplementary Fig. 11. Silencing hRNase 1 reduces EphA4-promoted spheroid formation and CD44⁺CD24⁻ cell population. **a**, WB of ZR-75-1 control cells (NEO-sh-Ctrl), ectopic EphA4 expressing ZR-75-1 cells (A4-sh-Ctrl), and ZR-75-1-A4 knockdown hRNase 1 cells (A4-sh-R1#1 and A4-sh-R1#2) blotted with EphA4 and hRNase 1 antibodies. **b**, Representative images of primary spheres of the indicated ZR-75-1 stable clones from (a). Bar, 100 μ m. **c**, WB of BT-474 control cells (NEO-sh-Ctrl), ectopic EphA4 expressing BT-474 cells (A4-sh-Ctrl), and BT-474-A4 knockdown hRNase 1 cells (A4-sh-R1#1 and A4-sh-R1#2) blotted with EphA4 and hRNase 1 antibodies. **d**, Representative images of primary spheres of the indicated BT-474 stable clones from (c). Bar, 100 μ m. **e**, Quantification of spheroid formation assay of the indicated BT-474 stable clones. One-tailed p values are shown. NEO-sh-Ctrl vs A4-sh-Ctrl, *p = 0.0176, A4-sh-Ctrl vs A4-sh-R1#1, *p = 0.0456, A4-sh-Ctrl vs A4-sh-R1#2, **p = 0.0066. **f**, Flow cytometric analysis of membrane CD44 and CD24 expression of the indicated BT-474 stable clones. **g**, Quantification of flow cytometric analysis from (f). NEO-sh-Ctrl vs A4-sh-Ctrl, **p = 0.0033, A4-sh-Ctrl vs A4-sh-R1#1, *p = 0.0200, A4-sh-Ctrl vs A4-sh-R1#2, **p = 0.0011. **h**, WB of EphA4 and hRNase 1 in KPL4 control cells (KPL4-NEO), ectopic EphA4 expressing KPL4 cells (KPL4-A4), and KPL4-A4 knockout hRNase 1 (KO-R1) or control (KO-Ctrl) cells. **i**, Flow cytometric analysis of membrane CD44 and CD24 expression in KPL4 cells as indicated. The percentages of CD44⁺CD24⁻ cells are shown in the lower right quadrant of each panel. **j**, Quantification of flow cytometric analysis from (i). NEO vs A4, *p = 0.0182, A4-KO-Ctrl vs A4-KO-R1, *p = 0.0110. All error bars represent mean \pm SD. Data represent two (a, c, h) or three (b, d, e, g, j) independent experiments. *p < 0.05, **p < 0.01, unpaired t test, one-tailed (e) and two-tailed (g, j). Source data are provided as a Source Data file.



Supplementary Fig. 12. Silencing EphA4 reduces hRNase 1-mediated spheroid formation. a, WB of MCF7 control cells (NEO-sh-Ctrl), hRNase 1 expressing MCF7 cells (R1-sh-Ctrl), and MCF7-R1 knockdown EphA4 cells (R1-sh-A4#1 and R1-sh-A4#2) blotted with EphA4 and

hRNase 1 antibodies. **b**, Representative images of primary spheres of the indicated MCF7 stable clones from **(a)**. Bar, 100 μ m. **c**, WB of EphA4 and hRNase 1 in BT-549 control cells (BT-549-NEO), hRNase 1 expressing BT-549 cells (BT-549-R1), and BT-549-R1 transfected with shRNA of two different sequences against EphA4 (sh-A4#1 and sh-A4#2) or with scrambled control (sh-Ctrl). **d**, WB of EphA4 and hRNase 1 in BT-549-NEO, BT-549-R1, and BT-549-R1 knockout EphA4 (KO-A4) or control (KO-Ctrl) cells. **e**, Quantification of soft agar colony formation assay of the indicated BT-549 stable clones from **(c)**. NEO vs R1, ***p = 0.0002, R1-sh-Ctrl vs R1-sh-A4#1, **p = 0.0021, R1-sh-Ctrl vs R1-sh-A4#2, ***p = 0.0006. **f**, Quantification of spheroid formation assay of the indicated BT-549 stable clones from **(c)**. NEO vs R1, **p = 0.0019, R1-sh-Ctrl vs R1-sh-A4#1, ***p = 0.0008, R1-sh-Ctrl vs R1-sh-A4#2, **p = 0.0012. The experiments were repeated once **(a, c, d)** and twice **(b)** with similar results. Data are representative of three independent experiments in triplicate **(e, f)**. All error bars represent mean \pm SD. **p < 0.01, ***p < 0.001, two-tailed unpaired t test. Source data are provided as a Source Data file.

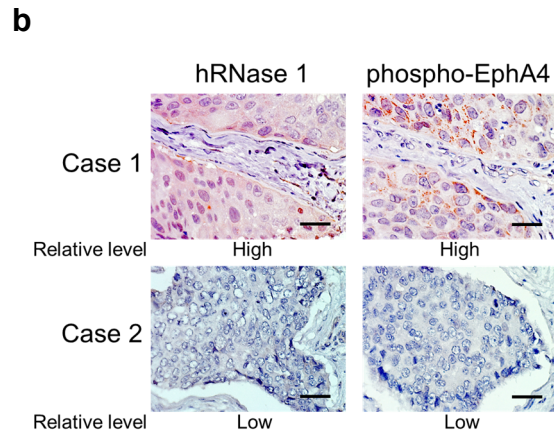


Supplementary Fig. 13. RNase 1-EphA4 axis contributes to breast tumorigenesis. **a** and **b**, WB analysis of mouse 4T1 mammary tumor cells expressing mouse RNase 1 (mRNase 1) and vector control blotted with antibodies against Flag (**a**) or RNase 1 (**b**; Santa Cruz Biotechnology, #sc-169198). The experiments were repeated an additional time with similar results. **c**, Tumor weight analysis (top) and representative images (bottom) of mice subcutaneously injected with the indicated 4T1 cells in (**a**) followed by treatment with solvent or compound 1 (cpd1). Bar, 1 cm. $n = 8$ per group except for the mRNase 1 group ($n = 6$). Vector vs mRNase 1, $**p = 0.0089$, mRNase 1 vs mRNase 1 + cpd1, $*p = 0.0264$. Error bars represent mean \pm SEM. $*p < 0.05$, $**p < 0.01$, ns, not significant, one-tailed unpaired t test. Source data are provided as a Source Data file.

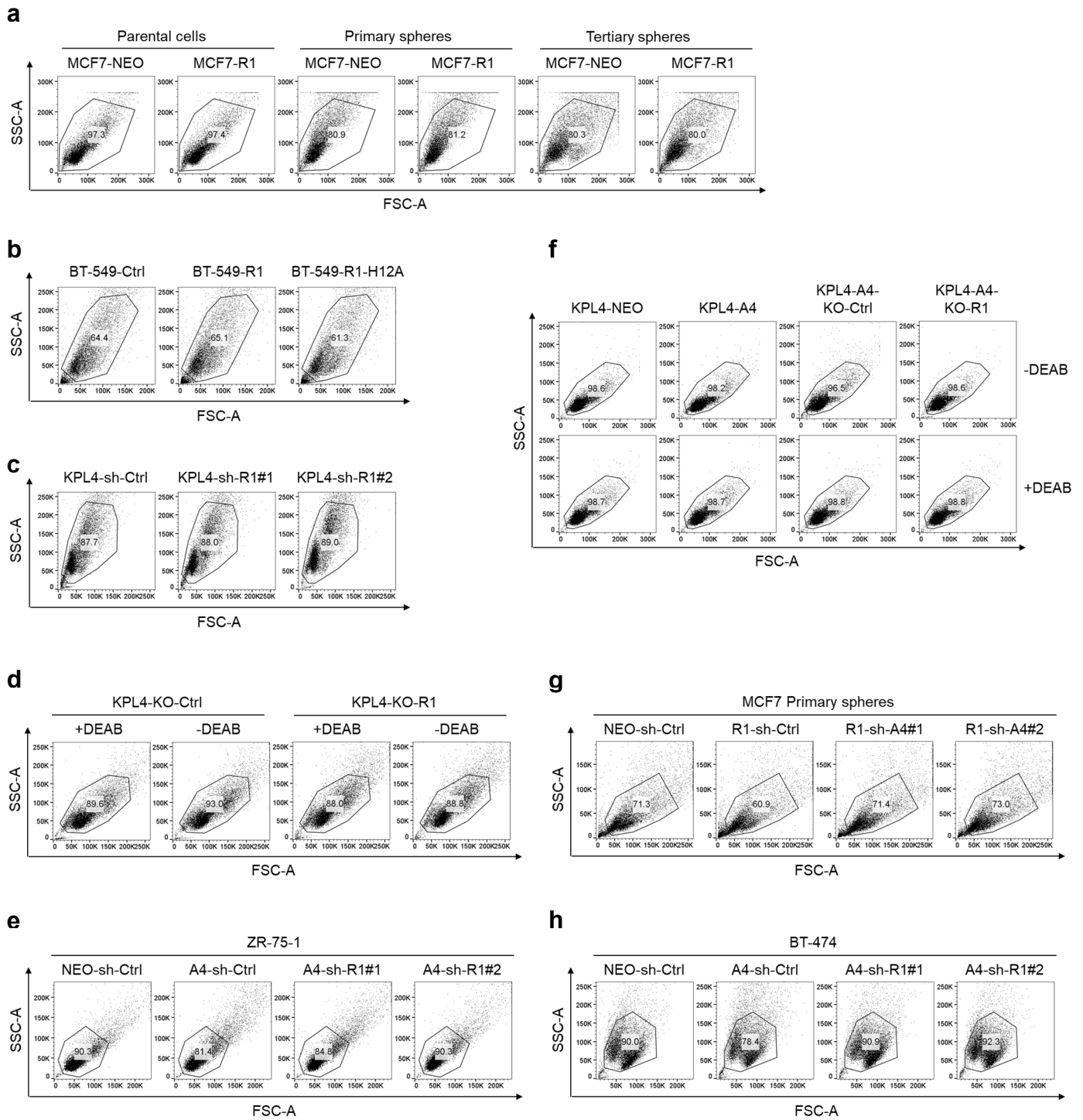
a

		phospho-EphA4		
		Low	High	Total
hRNase 1	Low	16	8	24
	High	4	20	24
	Total	20	28	48

p = 0.0001



Supplementary Fig. 14. Pathological relevance between hRNase 1 expression and EphA4 activation in breast cancer. a, Quantification of IHC staining for the correlation between hRNase 1 and phospho-EphA4-Y779 using human breast tumor tissue microarray analysis (Pantomics Inc., #BRC961; Pearson Chi-Square test). **b,** Two representative cases of IHC staining from (a). The experiment was repeated a second time with similar results. Bar, 50 μ m.



Supplementary Fig. 15. Gating strategies based on FSC-A/SSC-A parameters used for flow cytometric analysis of CD24/CD44 expression and ALDEFLUOR assay. a, Gating strategy to

determine the percentage of CD24⁻/CD44⁺ cells in the indicated MCF7 stable clones (parental cells) and primary and tertiary spheres derived from the indicated MCF7 stable clones presented on Fig. 2c. **b**, Gating strategy to determine the percentage of CD24⁻/CD44⁺ cells in BT-549 stable clones presented on Fig. 2f. **c**, Gating strategy to determine the percentage of CD24⁻/CD44⁺ cells in KPL4 stable clones presented on Fig. 2i. **d**, Gating strategy to determine the percentage of ALDEFUOR-positive cells by ALDEFUOR assay presented on Fig. 2m. **e**, Gating strategy to determine the percentage of CD24⁻/CD44⁺ cells in ZR-75-1 stable clones presented on Fig. 6b. **f**, Gating strategy to determine the percentage of ALDEFUOR-positive cells by ALDEFUOR assay presented on Fig. 6d. **g**, Gating strategy to determine the percentage of CD24⁻/CD44⁺ cells in primary spheres derived from the indicated MCF7 stable clones presented on Fig. 6h. **h**, Gating strategy to determine the percentage of CD24⁻/CD44⁺ cells in BT-474 stable clones presented on Supplementary Fig. 11f. Frequencies of cell population after gating are indicated in the gates.

Supplementary Table 1. A list of oligonucleotide primers used in the study

Name	Sequence
<i>For human RNase 1 cloning in pCDH-CMV-MCS-EF1 expression plasmid</i>	
pCDH-R1_F	ACGCGAATTCGCCACCATGGCTCTGGA
pCDH-R1_R	ACGCGGATCCTCACTTGTCGTCATCGTCTTTGTAG TCGGCGGTAGAGTCCTCCACAGA
<i>For human RNase 1 mutagenesis</i>	
R1-H12A_F	GGCAGGCTATGGACTCAGACAGTTCCC
R1-H12A_R	AGTCCATAGCCTGCCGCTGGAATTTCTTG
<i>For shRNA targeting human RNase 1</i>	
sh-R1#1 (V3LHS_313141)	TACAGTAGGTGGAGCTGCT
sh-R1#2 (V2LHS_32407)	TTGGTTACAGTAGGTGGAG
<i>For shRNA targeting human EphA4</i>	
sh-A4#1 (TRCN0000344511)	CCGGGACTTGCAAGGAGACGTTTAACTCGAGTTA AACGTCTCCTTGCAAGTCTTTTTG
sh-A4#2 (TRCN0000196950)	CCGGGACTTGCAAGGAGACGTTTAACTCGAGTTA AACGTCTCCTTGCAAGTCTTTTTG
<i>For knockout targeting human RNase 1 (KO-R1)</i>	
hRNase 1-1	TATTCGGGCGCCTCATCATT (271 to 293, – strand)
hRNase 1-2	CACCTTTGTGCACGAGCCCC (322 to 344, + strand)
hRNase 1-3	GTCTCTCCTTCGGGCTGGTC (481 to 503, – strand)
<i>For knockout targeting human EphA4 (KO-A4)</i>	
EphA4-1	TGTGGGAAGTGATGTCGTAC (2551 to 2573, + strand)
EphA4-2	GGCACCGGCGAACCATGGCT (97 to 119, + strand)
EphA4-3	CGACGCTGTCACAGGTTCCA (161 to 183, + strand)

Supplementary Table 2. A list of primary antibodies used in the study

Antibody	Supplier	Catalog No.	Appl.^a	Usage
Anti-Human β -Actin, clone AC-74	Sigma-Aldrich	#A2228	WB	1:10,000
Anti-Human Akt	Cell Signaling Technology	#9272	WB	1:1,000
Anti-Human Phospho-Akt (Ser473)	Cell Signaling Technology	#9271	WB	1:1,000
PE-Cy TM 7 Mouse Anti-Human CD24, Clone ML5	BD Biosciences	#561646	FC	1:100
APC Mouse Anti-Human CD44, Clone G44-26	BD Biosciences	#559942	FC	1:60
Anti-Human CD133 [EPR20980-104]	Abcam	#ab216323	IHC	1:200
Anti-Human Erk1/2	EMD Millipore	#06-182	WB	1:10,000
Anti-Human Phospho-Erk1/2 (Thr202/Tyr204) (D13.14.4E)	Cell Signaling Technology	#4370	WB	1:10,000
Anti-Human EphA3 (D-2)	Santa Cruz Biotechnology	#sc-514209	WB	1:500
Anti-Human EphA4 (N-terminal region), Clone M280	ECM Biosciences	#EM2801	WB	1:1,000
Anti-Human EphA4 (S-20)	Santa Cruz Biotechnology	#sc-921	PLA /IP	1:50 /4 μ g
Anti-Human EphA4 (6H7)	EMD Millipore	#AP1173	ELISA	3 μ g/ml
Anti-Human phospho-EphA4 (Y602)	ECM Biosciences	#EP2731	WB	1:1,000
Anti-Human phospho-EphA4 (Y779)	ECM Biosciences	#EP2751	WB	1:1,000
Anti-Human phospho-EphA4 (Y779/833)	LifeSpan BioSciences	#LS-C381624	IHC	1:150
Anti-Human EphA5 (L-15)	Santa Cruz Biotechnology	#sc-1014	WB /IP	1:500 /6 μ g
Anti-Human Ephrin-A1 (40-120 aa, Internal)	LifeSpan BioSciences	#LS-C383378	WB	1:1,000
Anti-Human Ephrin-A2 (C-Terminus)	LifeSpan BioSciences	#LS-C352139	WB	1:1,000
Anti-Human Ephrin-A3 [N1C3]	GeneTex	#GTX101455	WB	1:500
Anti-Human Ephrin-A4	R & D Systems	#AF369	WB	1:1,000
Anti-Human Ephrin-A5	R & D Systems	#AF3743	WB	1:1,000

Anti-Human Ephrin-A5 (Biotin, aa21-203)	LifeSpan BioSciences	#LS-C688235	ELISA	1:500
Anti-Human Ephrin-B1	Proteintech	#12999-1-AP	WB	1:1,000
Anti-Human Ephrin-B2 [N1C1]	GeneTex	#GTX105582	WB	1:1,000
Anti-Human Ephrin-B3	R & D Systems	#MAB395	WB	1:500
Monoclonal ANTI-FLAG® M2 antibody produced in mouse	Sigma-Aldrich	#F3165	WB /PLA	1:3,000 /1:100
Anti-GST (91G1)	Cell Signaling Technology	#2625	WB	1:3,000
Anti-Myc Tag, clone 4A6	EMD Millipore	#05-724	WB	1:3,000
Anti-Human p50 (E-10)	Santa Cruz Biotechnology	#sc-8414	WB	1:1,000
Anti-Human p65 (D14E12)	Cell Signaling Technology	#8242	WB	1:1,000
Anti-Human Phospho-p65 (S536) (93H1)	Cell Signaling Technology	#3033	WB	1:1,000
Anti-Human PLCγ1	Cell Signaling Technology	#2822	WB	1:1,000
Anti-Human Phospho-PLCγ1 (Y783)	Sigma-Aldrich	#SAB4503827	WB	1:1,000
Anti-Human RNase1	Sigma-Aldrich	#HPA001140	WB /IHC	1:1,000 /1:100
Anti-Human RNase1 (Biotin, aa29-156)	LifeSpan BioSciences	#LS-C299825	ELISA	1:500
Anti-Mouse RNase 1 (T-12)	Santa Cruz Biotechnology	#sc-169198	WB	1:1,000
Anti-Human Src (36D10)	Cell Signaling Technology	#2109	WB	1:1,000
Anti-Human Phospho-Src Family (Tyr416) (D49G4)	Cell Signaling Technology	#6943	WB	1:1,000
Anti-Human Tubulin, clone B-5-1-2	Sigma-Aldrich	#T5168	WB	1:10,000

^aELISA, Enzyme-Linked Immunosorbent Assay; FC, Flow Cytometry; IHC, Immunohistochemistry; IP, Immunoprecipitation; PLA, Proximity Ligation Assay; WB, Western Blotting.